IJDI-ERET

INTERNATIONAL JOURNAL OF DARSHAN INSTITUTE ON ENGINEERING RESEARCH AND EMERGING TECHNOLOGIES
Vol. 12, No. 2, 2023
www.ijdieret.in

(Research Article)

Mitigating Bend Pipe Erosion with the Incorporation of Twisted Tape Inserts

Yogendra Yadawa[1*]

[1]Department of Chemical Engineering and Biochemical Engineering, Rajiv Gandhi Institute of Petroleum Technology, Jais, Amethi, Uttar Pradesh, INDIA*

Abstract

Erosion poses a significant challenge across various industries, including thermal power plants and oil refineries. In this study, we employed commercial Computational Fluid Dynamics (CFD) software, ANSYS-FLUENT, to explore the impact of inserting a twisted tape at different axial locations upstream of the pipe's flow. Our investigation focused on the influence of average particle size and inlet velocity on erosion patterns at these various tape positions. Our findings reveal that the introduction of a twisted tape induces a swirling motion in the upstream section of the pipe. This swirling motion leads to a reduction in maximum momentum within the pipe's elbow, consequently diminishing the erosion rate in that specific region. Additionally, a noteworthy discovery is that, despite the twisted tape itself being susceptible to erosion, the erosion rate within the elbow decreases as the insertion point of the tape is positioned further upstream of the elbow.

Keywords: Standard elbow, twisted tape, elbow erosion, Ansys, erosion rate.

1. Introduction

Besides the energy consumptions, erosion is the impact of erodent particles on the solid surface caused by the removal of mass from the solid surface [1]. Several oil and gas corporations are quite concerned about erosion. Erosion occurs when the sand produced along with the oil and gas impacts pipe walls, couplings, and valves [2]. Thereby, based on erosion there are several most acceptable wear theories are the abrasive model [3], adhesive approximation [4], delamination theory [5] and rolling wear model [6]. Furthermore, metal oxide-based nanoparticles as well as nanotubes, nanorods, and nanofibers were also used to the removal of organic pollutants [7].

In the slurry flows, erosion wear and particle communication are complementary phenomena in which the primary mechanism for releasing energy is the formation of new surfaces [8].

Slurry transport through pipelines is a modern technology for transporting large amounts of slurry across long distances [9]. Henceforth, several approaches can be employed to examine erosion wear in standard elbows (without twisted tape) [10, 11]. In line with the studies conducted by Duart et al. [12, 13] and Pereira et al. [14], it is evident that the Oka model stands out as the most precise and reliable method. This preference arises from its foundation on measurable properties of both the eroded material and the erodent material [15].

Nonetheless, there exist several alternative methods, such as the insertion of a spiral wire or twisted tape in the upstream section of the bend pipe, which can effectively mitigate bend erosion caused by solid particles [16]. The twisted tape is used to diminish the erosion rate in pipelines flow [17].

Furthermore, gaining insight into the impacts of incorporating twisted tape into pipeline systems can enable its utilization as a passive control mechanism to mitigate undesired elbow erosion. This approach not only holds the potential to reduce maintenance expenses but also offers an alternative to costly measures like replacing the eroded curved sections. Subsequently, a twisted tape is introduced into the original geometry, specifically the standard elbow, while maintaining its inherent characteristics, including curvature radius and diameter. The computational fluid dynamics (CFD) simulation parameters, such as initial velocity, viscosity, and density, are also retained. This study places a particular emphasis on assessing the erosion rate reduction achieved by varying the insertion positions of the twisted tape upstream of the elbow [18].

2. Numerical Approaches and Erosion Prediction Models

In this investigation, the Euler-Lagrange method is used. Therefore, for the CFD analysis of twisted tape inserted in

[*]Corresponding Author: e-mail: pms19002@rgipt.ac.in, Tel-+91-7052589044
ISSN 2320-7590 (Print) 2583-3863 (Online)

bend pipe both phases of modelling such as gaseous phase model and particle motion models were discussed.

2.1 Gaseous phase model: In these experiments, an Unsteady-Reynolds-Averaged Navier-Stokes technique (URANST) [18] is used in the gaseous phase model and these model equations are given below by equations 1 and 2:

$$\frac{\partial_{(\rho u_i)}}{\partial_{(\chi_i)}} = 0 \tag{1}$$

$$\frac{\partial}{\partial t}(\rho u_i) + \frac{\partial}{\partial \chi_j}(\rho u_i u_j) = -\frac{\partial p}{\partial \chi_i} + \frac{\partial}{\partial \chi_j}\left[(\mu\ \mu_t)\left(\frac{\partial u_i}{\partial \chi_j} + \frac{\partial u_j}{\partial \chi_i}\right)\right] + Su_{ip} + \rho g_i \tag{2}$$

In this context, ρ represents the density of the fluid, u_i stands for the Reynolds-averaged velocity component, p signifies the mean pressure, μ denotes the dynamic viscosity of the gas, and μ_t represents the turbulent viscosity. Additionally, there are additional source terms attributed to phase interactions, which are denoted as Su_{ip}.

The advective term was calculated employing the second-order upwind technique, while the diffusive terms within the momentum equations and turbulence model equations were computed using the centered differencing scheme. One of the most renowned and extensively applied two-equation eddy viscosity models is the standard k-ε model [19]. It is worth noting that its initial development aimed to improve upon the mixing-length model and move beyond the algebraic specification of turbulence length scales in intricate flow scenarios. The turbulence kinetic energy (k) and its dissipation rate (ε) are treated as two scalar attributes of turbulence [18]:

$$\frac{\partial}{\partial t}(\rho k) + \frac{\partial(\rho u_j k)}{\partial \chi_j} = \frac{\partial}{\partial \chi_j}\left[\left(\mu + \frac{\mu_t}{\sigma_k}\right)\frac{\partial k}{\partial \chi_j} + P - \rho\varepsilon \tag{3}$$

$$\frac{\partial}{\partial t}(\rho k) + \frac{\partial(\rho u_j k)}{\partial \chi_j} = \frac{\partial}{\partial \chi_j}\left[\left(\mu + \frac{\mu_t}{\sigma_k}\right)\frac{\partial k}{\partial \chi_j} + P - \rho\varepsilon \tag{4}$$

Where P is the production term, which is given by:

$$P = (\mu_t + \mu)\left[\left(\frac{\partial u_i}{\partial \chi_j} + \frac{\partial u_j}{\partial \chi_i}\right)\frac{\partial u_i}{\partial \chi_j}\right] \tag{5}$$

The eddy viscosity in the conventional k-ε model is determined by Equation 6, which is derived from the turbulent kinetic energy (k) and turbulent dissipation rate (ε).

$$\mu_{t,standard} = C_{\mu\rho}\frac{k^2}{\varepsilon} \tag{6}$$

2.2 Particle motion model: In a Lagrangian framework, the dispersed phase is accounted for, where each particle is individually traced throughout the domain, and its equation of motion adheres to Newton's second law. For a rigid, spherical particle, the equations governing its trajectory, conservation of linear momentum, and conservation of angular momentum are presented below [18]:

$$\frac{d\chi_{pi}}{dt} = u_{pi} \tag{7}$$

$$m_p\frac{du_{pi}}{dt} = m_p\frac{3\rho C_D}{4\rho_p d_p}(u_i - u_{pi}) + F_{si} + F_{ri} + \left(1 - \frac{\rho}{\rho_p}\right)m_p g_i \tag{8}$$

$$I_p\frac{d\omega_{pi}}{dt} = T_i \tag{9}$$

In the equations mentioned above, $u_i = U_i + u_i'$ represents the components of the instantaneous fluid velocity. The average fluid velocity, U_i is obtained through interpolation from the resolved flow field, while the fluctuating component, u_i' is determined using the Langevin dispersion model. Here, d_p signifies the particle diameter, and $I_p = 0.1\ m_p\ d_p^2$ represents the moment of inertia for a spherical particle.

2.3 Erosion prediction model: As mentioned earlier, Pereira et al. [14] observed that the erosion ratio models proposed by Oka et al. [15] and the coefficient of restitution models by Grant and Tabakoff [20] were integrated to create the most appropriate erosion prediction method when analyzing 90-degree elbows. However, it's important to note that the erosion rate is defined as the mass of material removed per unit of area per unit of time. Consequently, the erosion rate is computed on the walls by aggregating the damage caused by each particle upon interacting with the wall surface [18], and this calculation is performed using Equation 10:

$$E_f = \frac{1}{A_f}\sum \dot{m_\pi}\, e_r \tag{10}$$

In the provided above equation A_f denotes the surface area exposed to erosion, $\dot{m_\pi}$ represents the mass flow rate of particles associated with each computational particle that impacts the surface, and e_r stands for the erosion ratio and it is defined as the ratio of the mass of eroded material to the mass of the erodent material.

3. Modelling of Geometry

3.1 Geometrical configuration of bend pipe with twisted tape: The geometrical configuration of the bend pipe with twisted tape were given below in tabular forms [18]:

Table 1. Elbow and twisted tape geometry specifications with simulation condition for erosion predictions

Geometry specifications		Simulation condition	
Pipe diameter (d)	25.0 mm	Fluid	Air
Inlet pipe length	1220 mm	Fluid density	1.2 kg/m^3
Outlet pipe length	101.4 mm	Fluid viscosity	0.0000179 Pa.s
Elbow curvature & bend angle	36.0 mm & 90°	Fluid velocity at inlet	30.1 m/s
Twisted tape thickness	25.2 mm	Specimen materials	Aluminium
Twisted tape length	76.2 mm	Materials density	2700 kg/m^3
Tape twisted angle	180º	Particle type	Angular SiO_2
Twisted tape position from elbow	0d, 1d, 2d, 3d	Particle density	2600 2601 m^3

3.2 Geometry and meshing of twisted tape inserted bend elbow: Figure (a-d) shows the geometry of standard elbow, twisted tape inserted at inlet of flow, twisted tape inserted at inlet of bend pipe, and meshing of inserted twisted tape geometry respectively.

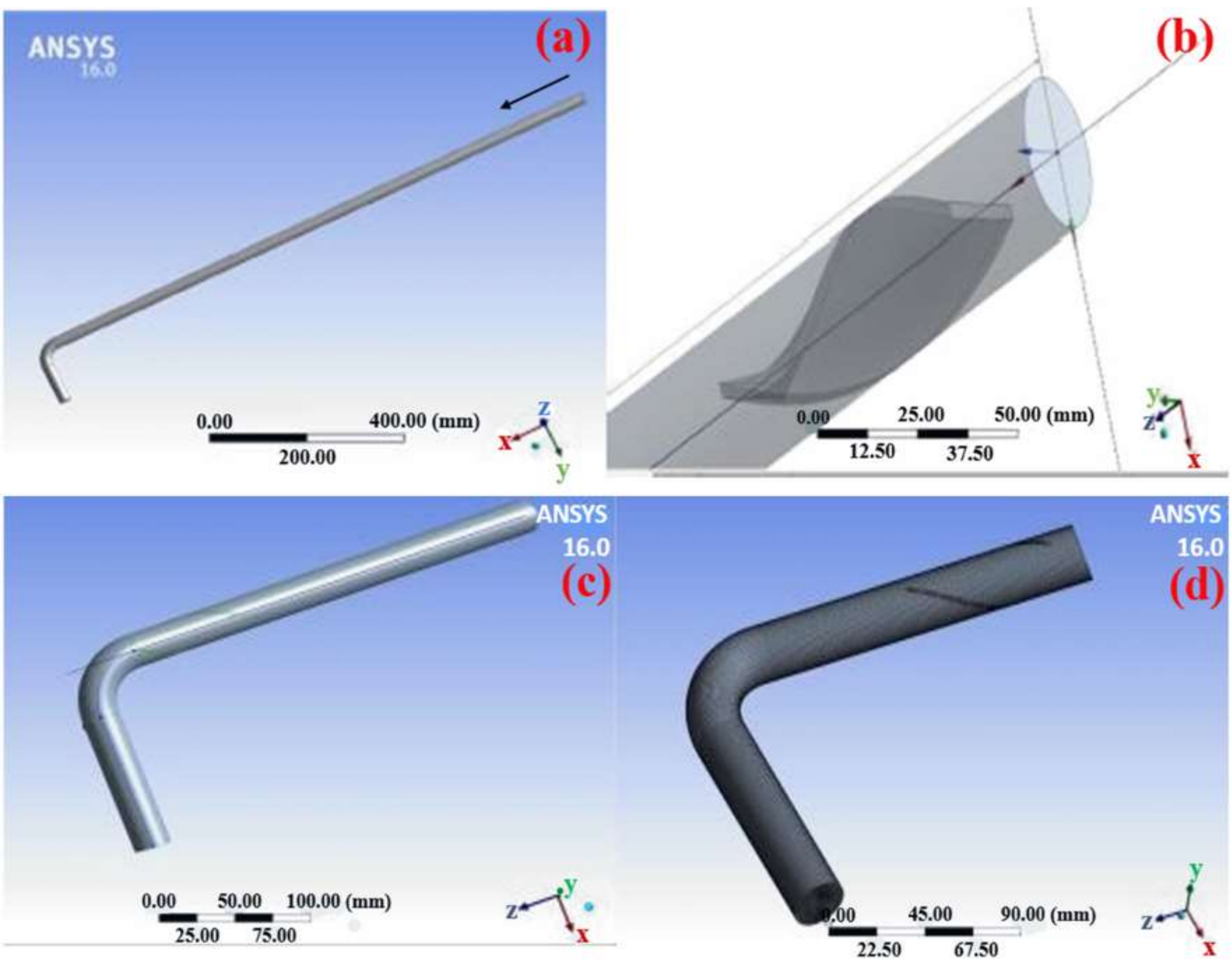

Figure 1. (a) Standard elbow (b) Twisted tape in inlet pipe (c) Twisted tape at inlet of bend pipe and (d) Meshing of inserted twisted tape geometry

3.3 Mesh generation: The generation of mesh in the form of structured grid was given below (table 2) as the tabular forms:

Table 2. Details of meshing

Grid type	Structured grid
Nodes	1371774
Elements	1314862
Element size	1.00 mm
Min. skewness	0.008
Max. skewness	0.554
Erosion model	Discrete phase model (DPM)

3.4 Boundary conditions: The boundary conditions and parameters used for the computational fluid dynamics were given below (Table 3) in tabular forms:

Table 3. Parameters used for CFD simulations

Pipe material	Aluminum (6061-T6)
Fluid	Air
Erodent particle	Silica sand
Turbulent model	Standard k-ε turbulence
Inlet velocity	30.10 m/s
Avg. particle size	180 µm (mean dia.)
Outlet pressure	Atm. gauge pressure
Erosion model	Discrete phase model (DPM)

4. Results and Discussion

4.1 Computational fluid dynamics (CFD) analysis for erosion rate: This section is divided into two parts, one is the computational fluid dynamics (CFD) for standard elbow (without inserted twisted tape), and second is the twisted tape inserted in bend pipe at different locations from the bend inlet. Subsequently, a twisted tape is introduced into the original pipeline at different locations, and the optimal position is identified to minimize bend erosion. Consequently, an analysis of the two-phase effects is conducted for this optimal position, and the results are compared to those obtained for the standard elbow. The comparison of maximum erosion rate predicted by the computational fluid dynamics data (CFD) and mathematical model (experimental data) were tabulated in Table 4.

Table 4: Comparison of maximum erosion rate (kg/m^2) predicted by the CFD data as well as experimental data

Elbow type	Particle size (µm)	V_{air} (m/s)	CFD data (kg/m^2)	Exp. Data (kg/m^2)	Error (%)
Standard elbow	180	30.1	$4.17 * 10^{-6}$	$3.25 * 10^{-6}$	22.06
Twisted tape inserted at 0D	180	30.1	$1.03 * 10^{-7}$	$6.39 * 10^{-8}$	37.96
Twisted tape inserted at 1D	180	30.1	$8.52 * 10^{-8}$	$5.93 * 10^{-8}$	30.39

The particles initially colloids with the twisted tape when they are introduced into the upstream pipeline, lose momentum, and then begin to be swirling motion. The bend wall has wider erosion outlines (Figure 2a), which protects it from more severe damage than would normally happen.

In Figure 2(a), it is evident that the erosion rate in the standard elbow experiences a reduction when the twisted tape is inserted into the inlet pipe. The erosion rate reaches its maximum value at a location 0d upstream of the elbow and exhibits the minimum erosion rate at a position 1d upstream of the elbow. Meanwhile, Figure 2(b) illustrates that when the twisted tape is inserted in the inlet pipe at a position 0d upstream of the elbow, the erosion rate within the elbow is notably lower compared to that of the standard elbow.

The maximum attainable velocity remains nearly consistent across all positions. However, the velocity profiles exhibit substantial variations depending on the placement of the twisted tape. Gas entering from the domain's inlet flows toward the insert, where it bifurcates along the length of the pipe, inducing a swirling motion. This swirling effect, caused by the twisted tape, persists for a certain length of the pipe, and the rotational motion gradually dissipates due to friction with the pipe and bend walls.

Additionally, as depicted in Figure 2(c), the erosion rate within the elbow is lower when the twisted tape is inserted into the inlet pipe at a position 1d upstream of the elbow, as compared to both the standard elbow and the configuration with the twisted tape inserted at 0d upstream of the elbow. Consequently, the insertion of the twisted tape at upstream positions (0d and 1d) of the inlet flow results in a reduction in the erosion rate.

4.2 Comparative analysis of erosion rate with and without twisted tape: Figure 3 presents a comparative analysis of erosion rates, considering both scenarios with and without a twisted tape inserted in the bend pipe. It is noteworthy that the placement of the twisted tape within the bend pipe extends progressively upstream in the direction of the inlet flow, with positions designated as 0D and 1D.

Moreover, Figure 3 highlights that the erosion rate in the standard pipe (without the presence of twisted tape) is notably higher when contrasted with the configuration where the twisted tape is inserted at various positions within the bend pipe. This difference is attributed to the incoming gas flow, which, upon reaching the twisted tape insert, divides into two segments along the length of the pipe. This division induces a swirling motion, ultimately leading to a reduction in the erosion rate [18].

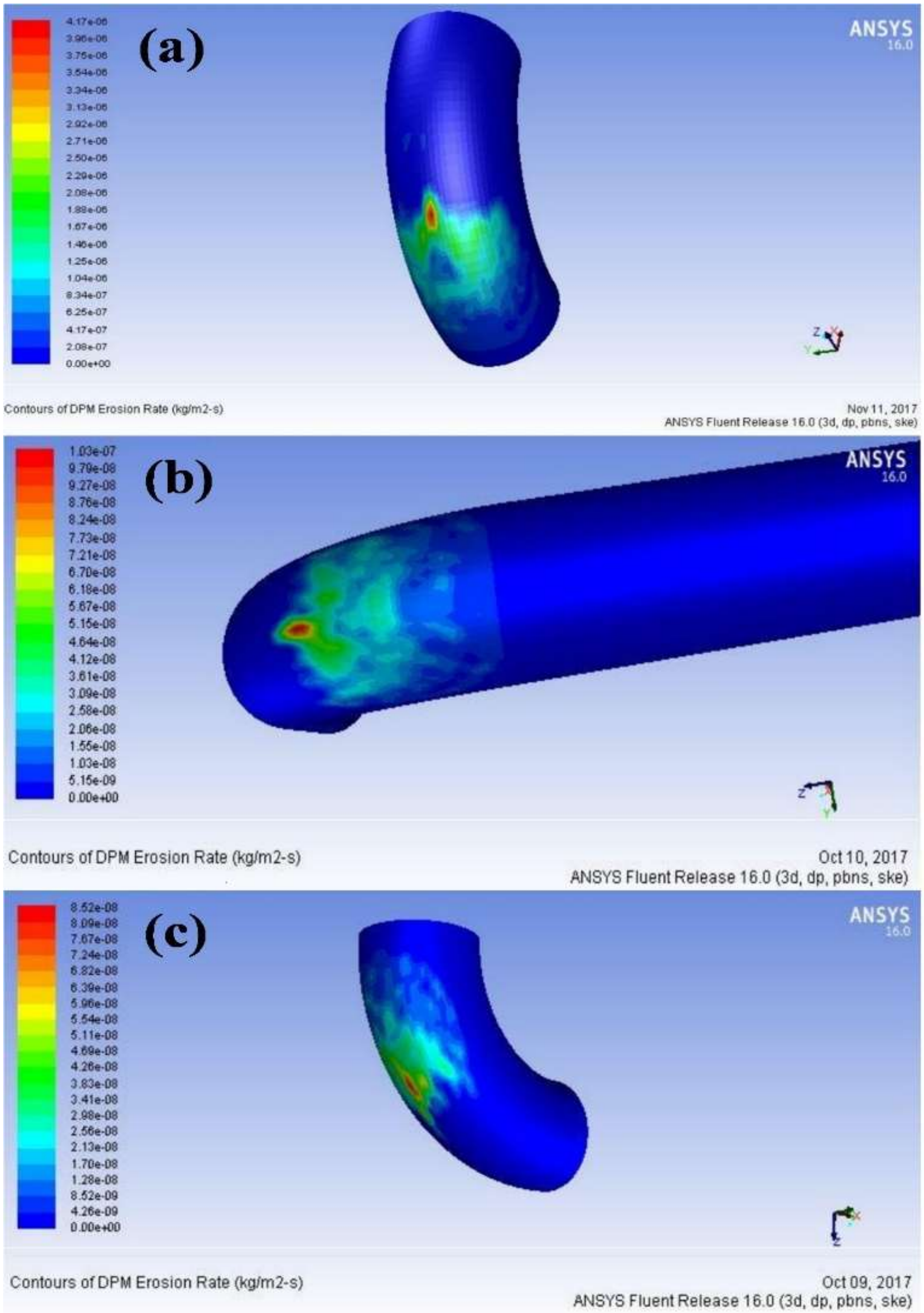

Figure 2. Erosion rate for **(a)** Standard elbows, **(b)** Twisted tape inserts at 0d position, and **(c)** Twisted tape inserts at 1d position from the bend pipe

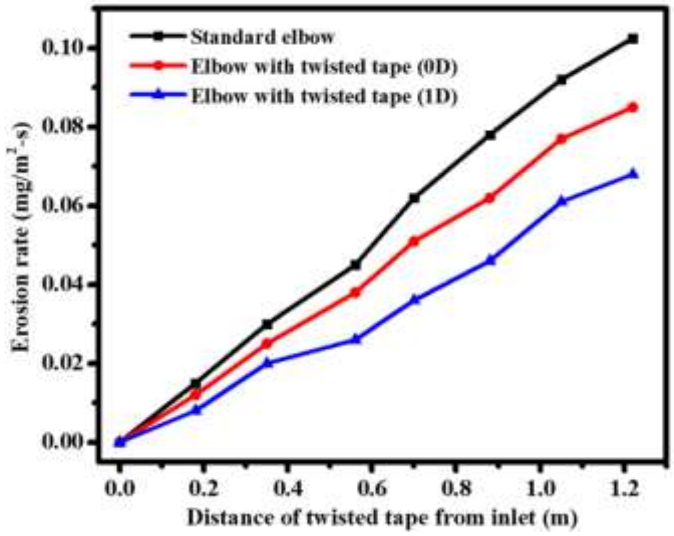

Figure 3. Erosion rate variation of standard elbow and twisted tape inserted in bend pipe at 0D and 1D position from the bend elbow

5. Conclusions

A numerical investigation was conducted to examine the impact of inserting twisted tape at various positions within a bend pipe. The findings suggest that the introduction of a twisted tape into a bend pipe effectively mitigates erosion rates. Notably, it was observed that the most favorable results were achieved when the tape was positioned farther from the bend's inlet, up to a distance of 1d. Beyond this point, placing the tape at even greater distances did not yield further improvements in erosion rate reduction.

Nomenclature

IJDI-ERET - International Journal of Darshan Institute on Engineering Research and Emerging Technologies
CFD - Computational Fluid Dynamics
URANST - Unsteady-Reynolds-Average-Navier-Stokes-Technique
DPM - Discrete Phase Model

Acknowledgement

Authors gratefully acknowledge the Department of Chemical and Biochemical Engineering, RGIPT, Jais, Amethi, India for providing the CFD software ANSYS-FLUENT facilities.

References

[1] P. J. Baker and B. E. A. Jacobs, *A guide to slurry pipeline systems*. BHRA Fluid Engineering, 1979.

[2] B. S. McLaury, J. Wang, S. A. Shirazi, J. R. Shadley, and E. F. Rybicki, “Solid Particle Erosion in Long Radius Elbows and Straight Pipes,” in *All Days*, San Antonio, Texas: SPE Annual Technical Conference and Exhibition, Oct. 1997, p. SPE-38842-MS. doi: 10.2118/38842-MS.

[3] R. C. D. Richardson, “The wear of metals by hard abrasives,” *Wear*, vol. 10, no. 4, pp. 291–309, Aug. 1967, doi: 10.1016/0043-1648(67)90093-2.

[4] J. T. Burwell and C. D. Strang, “On the Empirical Law of Adhesive Wear,” *Journal of Applied Physics*, vol. 23, no. 1, pp. 18–28, Jan. 1952, doi: 10.1063/1.1701970.

[5] N. P. Suh, “The delamination theory of wear,” *Wear*, vol. 25, no. 1, pp. 111–124, Jul. 1973, doi: 10.1016/0043-1648(73)90125-7.

[6] D. Berthe, L. Flamand, D. Foucher, and M. Godet, “Micropitting in Hertzian Contacts,” *Journal of Lubrication Technology*, vol. 102, no. 4, pp. 478–489, Oct. 1980, doi: 10.1115/1.3251583.

[7] Y. Yadawa, D. Jha, and N. Joshi, “Cost-effective efficient materials for dye degradation using non-aqueous sol–gel route,” *Environmental Science and Pollution Research*, Nov. 2023, doi: 10.1007/s11356-023-31036-z.

[8] M. C. Roco and G. R. Addie, “Erosion wear in slurry pumps and pipes,” *Powder Technology*, vol. 50, no. 1, pp. 35–46, Mar. 1987, doi: 10.1016/0032-5910(87)80081-5.

[9] A. Uzi, Y. Ben Ami, and A. Levy, “Erosion prediction of industrial conveying pipelines,” *Powder Technology*, vol. 309, pp. 49–60, Mar. 2017, doi: 10.1016/j.powtec.2016.12.087.

[10] K. R. Ahlert, “Effects of particle impingement angle and surface wetting on solid particle erosion of AISI 1018 steel | WorldCat.org,” The University of Tulsa, 1994. [Online]. Available: http://www.ecrc.utulsa.edu/StudentDissertations/ECRC%20Thesis/Kevin%20R.%20Ahlert%201994.PDF

[11] Y. Zhang, E. P. Reuterfors, B. S. McLaury, S. A. Shirazi, and E. F. Rybicki, “Comparison of computed

and measured particle velocities and erosion in water and air flows," *Wear*, vol. 263, no. 1, pp. 330–338, Sep. 2007, doi: 10.1016/j.wear.2006.12.048.

[12] C. A. R. Duarte, F. J. de Souza, and V. F. dos Santos, "Numerical investigation of mass loading effects on elbow erosion," *Powder Technology*, vol. 283, pp. 593–606, Oct. 2015, doi: 10.1016/j.powtec.2015.06.021.

[13] C. A. R. Duarte, F. J. De Souza, and V. F. Dos Santos, "Mitigating elbow erosion with a vortex chamber," *Powder Technology*, vol. 288, pp. 6–25, Jan. 2016, doi: 10.1016/j.powtec.2015.10.032.

[14] G. C. Pereira, F. J. De Souza, and D. A. De Moro Martins, "Numerical prediction of the erosion due to particles in elbows," *Powder Technology*, vol. 261, pp. 105–117, Jul. 2014, doi: 10.1016/j.powtec.2014.04.033.

[15] A. Venkatalaxmi, B. S. Padmavathi, and T. Amaranath, "A general solution of unsteady Stokes equations," *Fluid Dynamics Research*, vol. 35, no. 3, pp. 229–236, Sep. 2004, doi: 10.1016/j.fluiddyn.2004.06.001.

[16] D. Mills, *Pneumatic conveying design guide*, second. Amsterdam: Butterowrth-Heinemann, 2004. [Online]. Available: https://www2.hcmuaf.edu.vn/data/dh04cc/file/Pneumatic%20Conveying%20Design%20Guide.pdf

[17] R. J. K. Wood, T. F. Jones, N. J. Miles, and J. Ganeshalingam, "Upstream swirl-induction for reduction of erosion damage from slurries in pipeline bends," *Wear*, vol. 250, no. 1–12, pp. 770–778, Oct. 2001, doi: 10.1016/S0043-1648(01)00715-3.

[18] V. F. Dos Santos, F. J. De Souza, and C. A. R. Duarte, "Reducing bend erosion with a twisted tape insert," *Powder Technology*, vol. 301, pp. 889–910, Nov. 2016, doi: 10.1016/j.powtec.2016.07.020.

[19] J. E. Bardina, P. G. Huang, and T. J. Coakley, "Turbulence Modeling Validation, Testing, and Development," Apr. 1997, [Online]. Available: https://ntrs.nasa.gov/citations/19970017828

[20] G. Grant and W. Tabakoff, "Erosion Prediction in Turbomachinery Resulting from Environmental Solid Particles," *Journal of Aircraft*, vol. 12, no. 5, pp. 471–478, May 1975, doi: 10.2514/3.59826.

Biographical notes

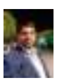

Yogendra Yadawa pursuing Ph.D. in the areas of Materials Science and Engineering from Rajiv Gandhi Institute of Petroleum Technology Jais Amethi in the Department of Chemical Engineering and Biochemical Engineering (CEBE) and received M.Tech. from MNNIT, Allahabad in Fluid Engineering. His research interest includes Metal Oxides Nanocomposites Materials, Nanofibers, Multiphase Flow.